



an ASME  
publication

Copyright © 1975 by ASME

\$3.00 PER COPY

\$1.00 TO ASME MEMBERS

The Society shall not be responsible for statements or opinions advanced in papers or in discussion at meetings of the Society or of its Divisions or Sections, or printed in its publications. *Discussion is printed only if the paper is published in an ASME journal or Proceedings.* Released for general publication upon presentation. Full credit should be given to ASME, the Technical Division, and the author(s).

## Observations of Separated Laminar Flow on Axial Compressor Blading

G. J. WALKER

Senior Lecturer,  
Department of Civil and Mechanical Engineering,  
University of Tasmania,  
Hobart, Tasmania, Australia  
Mem. ASME

This paper describes some detailed observations of separated laminar flow regions on the rotating and stationary blading of a single-stage axial compressor operating at low speed. The data covers the "critical" Reynolds number range where "bursting" of laminar separation bubbles causes a sharp increase in blade profile losses. The experimental results are compared with various empirical correlations and theoretical models proposed by other workers. Horton's semi-empirical model of separation bubble bursting is broadly supported by the present investigation. However, it appears that some aspects of Horton's theory require significant modification in order to give an accurate description of the separation bubble behavior on the blades in an axial compressor. It is stressed that correlations of the critical Reynolds number for axial compressor cascades in terms of overall performance parameters should be applied with caution, as they are only likely to be valid for a narrow range of conditions.

Contributed by the Gas Turbine Division of The American Society of Mechanical Engineers for presentation at the Gas Turbine Conference & Products Show, Houston, Texas, March 2-6, 1975. Manuscript received at ASME Headquarters December 2, 1974.

Copies will be available until December 1, 1975.

# Observations of Separated Laminar Flow on Axial Compressor Blading

G. J. WALKER

## INTRODUCTION

As the operating Reynolds number of an aerofoil is reduced, the location of boundary layer transition gradually moves rearwards, and separation of the laminar shear layer may eventually occur. Where laminar separation is quickly followed by transition and reattachment of the free turbulent shear layer, a small closed region of flow separation or "laminar separation bubble" will be formed. With further reduction in Reynolds number, the initially short separation bubble may suddenly increase in size or "burst," causing marked changes in the aerofoil performance and surface pressure distribution. The bursting phenomenon is responsible for the undesirable leading edge type of stall on isolated aerofoils; it also causes the sudden increase in losses observed when the Reynolds number of an axial compressor cascade is reduced below a certain "critical" value.

Early work on low-speed flows around isolated aerofoils with bubble separations has been reviewed by Tani (1).<sup>1</sup> Some detailed studies of separation bubbles generated on a flat plate have been reported by Young and Horton (2), Gaster (3), Woodward (4) and Horton (5). Various observations of flow separation and Reynolds number effects on cascades have been described by Blight and Howard (6, 7), Crooks and Howard (8), Rhoden (9), Stuart (10), Citavy and Norbury (11), Schlichting (12) and Roberts (13). Investigations of flow separation on axial compressor blades have mostly been limited to descriptions of changes in overall performance or surface pressure distributions, such as that given by Shaw (14); however, the writer (15, 16) has made a fairly detailed study of separated flow regions on the blading of a single-stage axial compressor. The only other detailed measurements of separation bubbles on compressor blades known to the writer are those of Evans (17).

<sup>1</sup> Underlined numbers in parentheses designate References at end of paper

This paper commences by outlining the flow mechanism in laminar separation bubbles, and reviewing various empirical and semi-empirical methods of predicting their growth and bursting. Some detailed measurements of laminar separation bubbles on axial compressor blades are then presented, and various modifications to Horton's model of the laminar separation bubble are suggested on the basis of these observations. In conclusion, the problem of correlating the critical Reynolds number for an axial compressor cascade is discussed.

## FLOW MECHANISM IN SEPARATION BUBBLES

A diagram of the flow mechanism in a short two-dimensional laminar separation bubble is given in Fig. 1. Over the forward part of the bubble, where the flow remains laminar, there is very little entrainment of fluid by the separated shear layer, and the velocity of reverse flow underneath it is correspondingly small. This gives rise to an almost stagnant, or "dead air" region, which causes the surface pressure to remain almost constant, nearly equal to the pressure at separation.

Theoretical models of flow in separation bubbles usually assume instantaneous transition in the laminar shear layer, but it is more realistic to assume that transition to turbulent flow occurs over a finite distance. When transition commences, the rate of entrainment by the shear layer rapidly increases, and the mean flow streamlines curve back towards the bounding surface. The dividing streamline turns over sharply and returns to the surface at the reattachment point to close the bubble. Continuity requires a much higher reverse flow velocity under the separated turbulent shear layer because of the faster rate at which fluid is entrained by the turbulent flow.

In the rearward part of the bubble, the flow is very unsteady because of the eddies reaching out from the spreading turbulent shear

## NOMENCLATURE

<p><math>c</math> = blade chord</p> <p><math>i</math> = incidence</p> <p><math>x</math> = streamwise distance</p> <p><math>x_1 = x_t - x_i</math> = length of unstable laminar flow</p> <p><math>x_1 = x_T - x_S</math> = length of separated laminar shear layer</p> <p><math>x_2 = x_R - x_T</math> = length of separated turbulent shear layer</p> <p><math>p</math> = static pressure</p> <p><math>x</math> = chordwise distance from leading edge</p> <p><math>A</math> = parameter depending on surface pressure distribution</p> <p><math>B</math> = parameter depending on surface pressure distribution</p> <p><math>C_d</math> = dissipation coefficient</p> <p><math>C_p</math> = static pressure coefficient</p> <p><math>D</math> = overall diffusion factor</p> <p><math>H = \delta^*/\theta</math> = boundary layer shape factor</p> <p><math>H_e = \epsilon/\theta</math> = boundary layer shape factor</p> <p><math>P = (\theta^2/\nu) (\Delta U/\Delta x)</math> = pressure gradient parameter for laminar separation bubble</p> <p><math>Re_b</math> = chord Reynolds number at bursting</p> <p><math>Re_c = U_\infty c/\nu</math> = blade Reynolds number</p> <p><math>Re_{s1} = U_{s1}/\nu</math> = Reynolds number based on length of separated laminar flow</p> <p><math>Re_{\delta^*} = U\delta^*/\nu</math> = boundary layer Reynolds number</p> <p><math>Re_\theta = U\theta/\nu</math> = boundary layer Reynolds number</p> <p><math>U</math> = velocity at outer edge of boundary layer</p> <p><math>U_{mb}</math> = rotor velocity at mid-blade height</p> <p><math>U_c</math> = vector mean velocity for a cascade</p>	<p><math>\bar{v}_a</math> = mean axial velocity</p> <p><math>\Delta x = x_R - x_S</math> = length of laminar separation bubble</p> <p><math>\Delta U = U_R - U_S</math> = change in free stream velocity over laminar separation bubble</p> <p><math>\beta_1</math> = direction of camber line at leading edge (to axial)</p> <p><math>\beta_2</math> = direction of camber line at trailing edge (to axial)</p> <p><math>\delta^*</math> = displacement thickness</p> <p><math>\epsilon</math> = kinetic energy thickness</p> <p><math>\theta</math> = momentum thickness</p> <p><math>\mu_t</math> = dynamic eddy viscosity</p> <p><math>\nu</math> = kinematic viscosity</p> <p><math>\rho</math> = density</p> <p><math>\sigma = (p_R - p_S)/\frac{1}{2} \rho U_S^2</math> = pressure rise parameter for laminar separation bubble</p>
	<p style="text-align: center;"><u>Subscripts</u></p> <p><math>b</math> = value at bursting</p> <p><math>i</math> = value at point of neutral stability to small two-dimensional disturbances in laminar boundary layer</p> <p><math>m</math> = mean value over unstable laminar flow region</p> <p><math>t</math> = value at point where turbulent flow first appears</p> <p><math>R</math> = value at turbulent reattachment point</p> <p><math>S</math> = value at laminar separation point</p> <p><math>T</math> = value at instantaneous transition point assumed in Horton's model</p> <p><math>T</math> = value at point where flow becomes wholly turbulent</p>

layer, and there is a zone of vigorous recirculation which limits the downstream extent of the dead air region. A strong rise in surface pressure is required to balance the inertia forces generated by the curvature of the mean streamlines in the reversing flow immediately upstream of the reattachment point. The pressure continues to rise rapidly for a short distance after reattachment due to the boundary layer displacement thickness initially tending to decrease.

After a short bubble has burst to form a "long" bubble, a somewhat different flow behavior

is observed. As noted by Woodward (4), the separated shear layer in a long bubble bends over much more smoothly and continuously to effect reattachment; the point at which the surface pressure commences to rise may then be well downstream of the transition region in the separated shear layer. In contrast to this, the reattachment process in a short bubble is much more rapid, and the commencement of surface pressure rise corresponds quite closely to the onset of the turbulent flow.

Short bubbles interact very little with

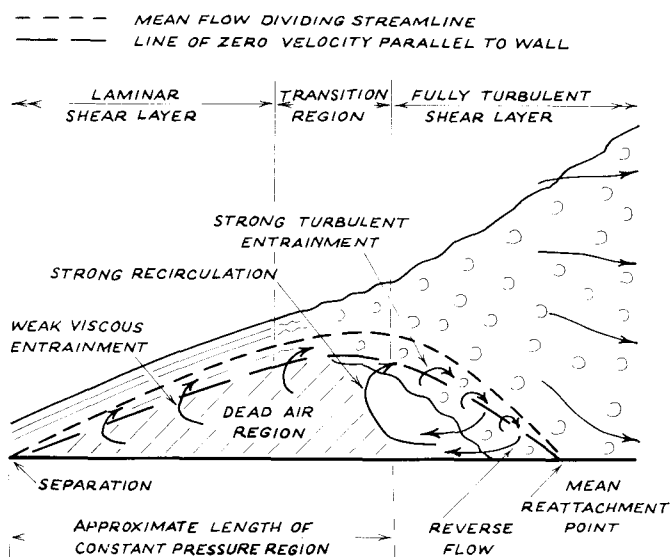


Fig. 1 Flow mechanism in a short two-dimensional laminar separation bubble

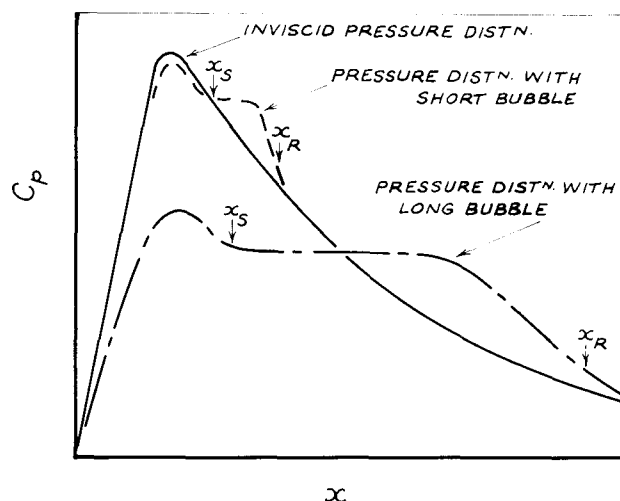


Fig. 2 Typical pressure distributions on an isolated aerofoil with different types of laminar separation bubbles

the external flow around an aerofoil, and cause only small perturbations to the surface pressure distribution. But long bubbles have a much more marked effect, tending to collapse the suction peak and reduce the lift. Typical forms of the suction surface pressure distribution on aerofoils with short and long bubbles near the leading edge are shown in Fig. 2.

#### PREVIOUS WORK ON LAMINAR SEPARATION BUBBLES

The earliest attempts to describe the behavior of laminar separation bubbles used correlations involving properties of the laminar boundary layer at separation. The philosophy underlying this approach was that bubble bursting might have been associated with a sudden change in flow stability causing a marked increase in length of the separated laminar shear layer.

Owen and Klanfer (18) analysed the results of tests on NACA 63-009 and 64-006 aerofoils, and suggested that bubbles would either be short, with a non-dimensional length  $l/\delta_S^* = 0[10^2]$ , or long, with  $l/\delta_S^* = 0[10^3 - 10^4]$ , depending on whether the boundary layer Reynolds number at separation,  $Re_{\delta_S^*}$ , was greater or less than about 450. Crabtree (19), however, noted that bursting appeared to occur at higher Reynolds numbers in some isolated cases observed by McGregor (20), and this led him to introduce an additional parameter

$$\sigma = (P_R - P_S) / \frac{1}{2} \rho U_S^2 = 1 - (U_R / U_S)^2 \quad (1)$$

based on the pressure rise over the bubble. Crabtree's hypothesis was that bursting would occur either through  $Re_{\delta_S^*}$  falling to 450, or by  $\sigma$  rising to a critical value of about 0.35, but this model gave only moderate agreement with experiment.

To obtain more data about the bursting problem, Gaster (3) carried out a series of detailed measurements on laminar separation bubbles formed on a flat plate under carefully controlled conditions. From the results obtained, he formulated a two-parameter bursting criterion based on the separation Reynolds number,  $Re_{\delta_S^*}$ , and the non-dimensional pressure gradient over the bubble,

$$P = (\delta_S^2 / \nu) (\Delta U / \Delta x) \quad (2)$$

Here,  $\Delta U = (U_R - U_S)$  is the change in free-stream velocity over the length of the bubble,  $\Delta x = x_R - x_S$ . Gaster's data indicated a unique relationship between the parameters,  $Re_{\delta_S^*}$  and  $P$ , at bursting, which can be seen in Fig. 7. It appeared from this result that Owen and Klanfer's single-parameter bursting criterion was a special case of the more general two-parameter criterion. Another notable feature of Gaster's measurements was that the separated flow regions on the flat plate underwent a gradual transition from the short to the long bubble regime, rather than the sudden bursting process observed on isolated aerofoils.

Wallis (21) followed a completely different approach by suggesting that bubble bursting occurred through separation of the reattached tur-

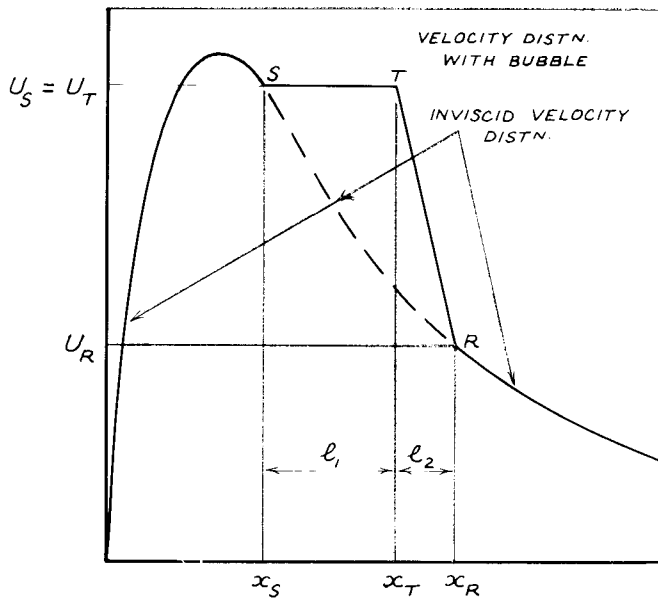


Fig. 3 Simplified model of a short laminar separation bubble -- after Horton (5)

bulent boundary layer downstream of the bubble, but this model did not enjoy early acceptance by other workers. However, the later investigations of Woodward (4, 22) and Horton (5) have now firmly established that bursting is caused by a failure of the turbulent shear layer to reattach. The invalidity of the laminar stability hypothesis for bubble bursting was demonstrated by Woodward (22), who observed transition to occur in very nearly the same physical position just before and just after bursting. It is noted that Gaster's bubble bursting boundary in the  $P \sim Re_{\delta}^*$  plane may be roughly approximated by a straight line through the origin; the equation to this line is

$$[(\theta/\delta^*) (\Delta U/\Delta x)]_b = \text{constant} \quad (3)$$

which may be crudely interpreted as a turbulent separation criterion.

#### Horton's Semi-Empirical Model

Following Woodward's suggestion that bubble bursting was associated with the behavior of the turbulent shear layer, Horton (5) sought to develop a criterion for turbulent reattachment analogous to existing boundary layer separation criteria. Using the momentum integral and kinetic energy integral equations, together with the assumption that the energy shape factor,  $H_e = \epsilon/\theta$ , passed through a minimum at the reattachment point gave the relation

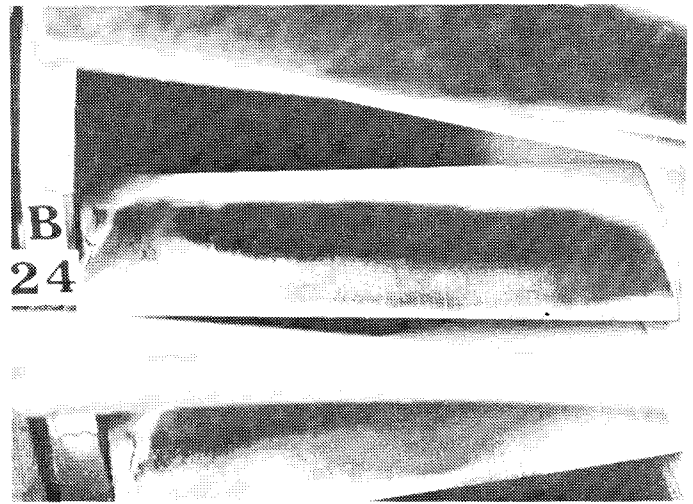


Fig. 4 China clay test on stator suction surface  $i = -6.2$  deg,  $Re_c = 1.72 \times 10^5$  at mid-blade height (viewed through rotor looking downstream; hub at right, tip at left)

$$[(\theta/U)(dU/dx)]_R = - [C_d/(H_e(H-1))]_R \quad (4)$$

where  $C_d$  is the turbulent dissipation coefficient and  $H = \delta^*/\theta$  is the velocity profile shape factor. Assuming a constant eddy viscosity specified by

$$\mu_t = 0.020 \rho U \delta^* \quad (5)$$

together with information derived from the measured velocity profile at reattachment gave

$$C_{dR} = 0.0222 \quad (6)$$

Substituting this into equation (5), together with mean empirical values of  $H = 3.50$  and  $H_e = 1.51$  for the reattachment profile yields the reattachment criterion

$$[(\theta/U)(dU/dx)]_R = -0.0059 \quad (7)$$

However, the experimental data analyzed by Horton gave a slightly different result from equation (7), indicating an average value of

$$[(\theta/U)/(dU/dx)]_R = -0.0082 \quad (8)$$

with a standard deviation of 0.0016. Horton

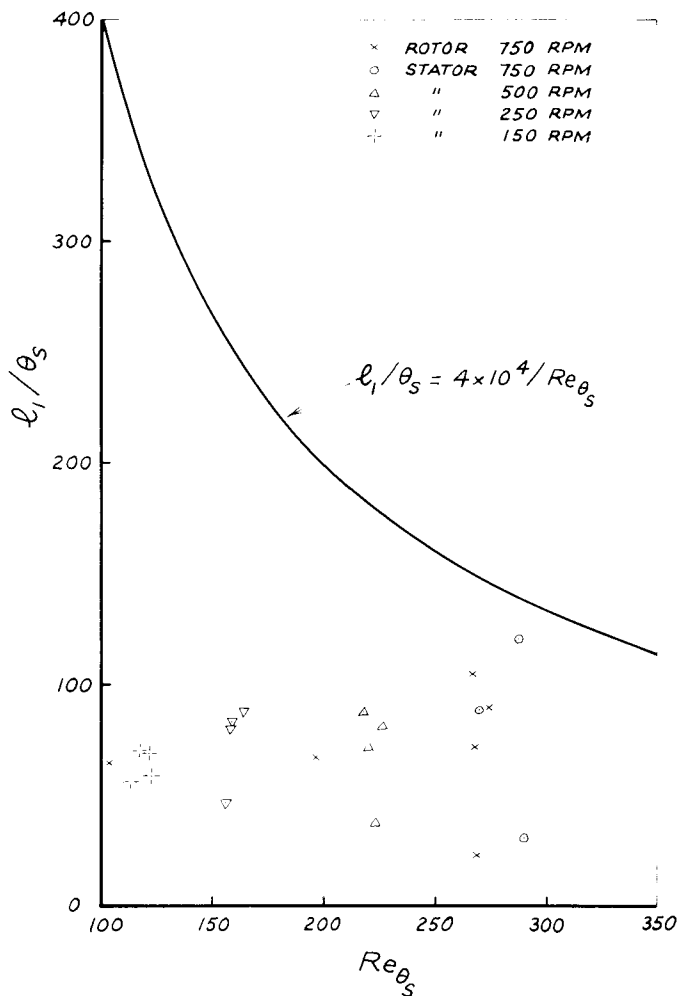


Fig. 5 Non-dimensional length of the dead air region in laminar separation bubbles on the rotor and stator blade suction surfaces

suggested that this could be explained by the rate of entrainment and the dissipation coefficient for a reattaching turbulent shear layer being rather higher than that for a corresponding attached layer.

Having developed a turbulent reattachment criterion, Horton proceeded to formulate a simple model for the growth and bursting of short laminar separation bubbles, based on the following assumptions:

1 An external velocity distribution in the neighborhood of the bubble as shown in Fig. 3. The commencement of pressure rise is coincident with the point of transition in the separated shear layer,  $x_T$  (transition being assumed to occur instantaneously);

2 A length of constant pressure region,  $l_1 = x_T - x_S$  (equal to the length of separated

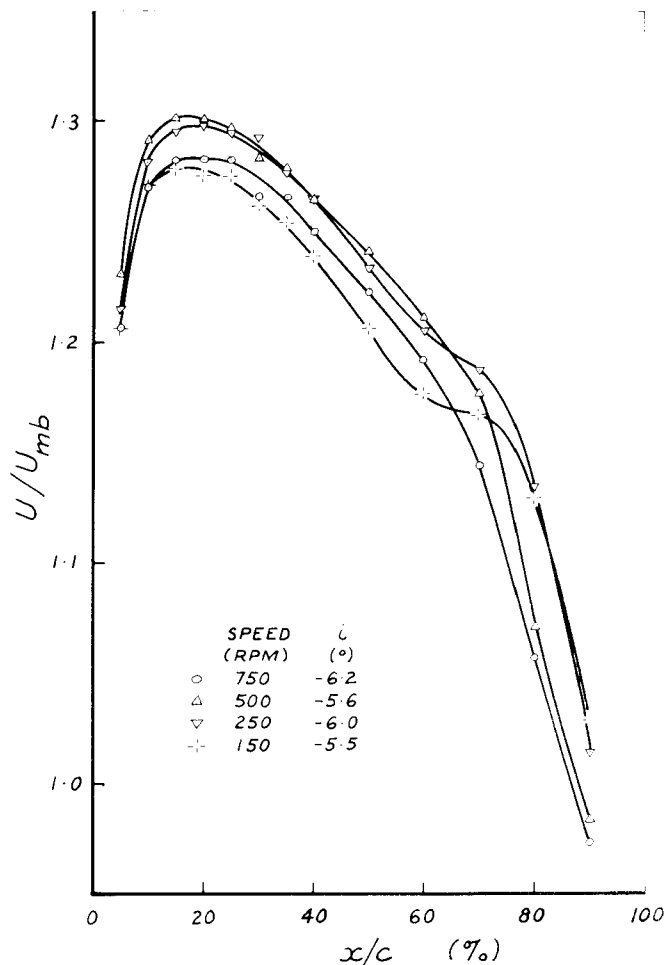


Fig. 6 Influence of Reynolds number on the stator blade suction surface velocity distribution at mid-blade height for  $\alpha \approx -6$  deg — showing effect of developing separated flow region (See Table 1 for location of separation, transition, and reattachment points).

laminar flow), given by the empirical correlation

$$l_1/\theta_S = 4 \times 10^4 / Re_{\theta_S} \quad (9)$$

The assumption of constant pressure gives

$$\theta_T = \theta_S \quad (10)$$

3 A value of  $(\theta/U) (dU/dx) = -0.0082$  at the point of turbulent reattachment,  $x_R$ , where the velocity gradient is taken as

$$(dU/dx)_R = (U_R - U_T)/(x_R - x_T) \quad (11)$$

Table 1

Shear Layer Behavior in Separation Bubbles on Stator  
Suction Surface at  $i = -6$  deg.

(See Fig. 6 for corresponding surface velocity distributions)

Speed (rpm)		(deg)	(percent)	(percent)	(percent)	(percent)
750	$1.72 \times 10^5$	-6.2	62	68	70	82
500	$1.13 \times 10^5$	-5.6	60.5	71	73	85
250	$5.57 \times 10^4$	-6.0	59	70	83	85
150	$3.24 \times 10^4$	-5.5	57	70	84	*

The predictions of this model were in good qualitative and fair quantitative agreement with experiment, and thus confirmed that bubble bursting was caused by a fundamental breakdown of the turbulent reattachment process.

OBSERVATIONS OF SEPARATION BUBBLES ON AXIAL COMPRESSOR BLADES

Experimental Detail

This section describes the writer's observations of separated flow regions on the blading of a single-stage axial compressor (15). The experimental techniques employed included the measurement of surface pressure distributions, and the use of china clay surface visualisation on both rotating and stationary blades. A hot wire anemometer was used to measure mean velocity profiles in the boundary layer, and separated flow regions on the suction surface of an outlet guide vane at mid-blade height. Surveys with a stethoscope connected to a total head tube were also carried out to assist in locating transition.

The compressor speed was varied from 150 to 750 rpm, giving values of chord Reynolds number,  $Re_c$ , for the outlet guide vanes (i.e. stators) in the range  $3 \times 10^4$  to  $2 \times 10^5$ . By changing the compressor throughflow, the stator incidence was varied from about  $-11$  to  $+5$  deg, while the rotor incidence ranged from about  $-11$  to  $+9$  deg at mid-blade height; this covered the flow range from just above surge to the maximum obtainable flow. Measurements of the streamwise velocity fluctuations near the stator leading edge indicated average values of 2 percent free stream turbulence at 750 rpm rising to 6 percent at 150 rpm; turbulence levels of around 10 percent were obtained near stall at 150 rpm. Values of

axial velocity ratio at mid-blade height measured by Oliver (23) at a compressor speed of 750 rpm ranged from 0.995 at maximum flow to 1.05 at stall for the rotor; the corresponding range of axial velocity ratio values for the stator was 1.02 to 1.065.

The axial flow compressor used in this investigation was designed and built at the Australian Department of Supply's Aeronautical Research Laboratories in Melbourne, and is now operated at the University of Tasmania in Hobart. Only brief details of this machine will be given here: a more complete description has been given by Oliver (23). Air enters radially through a cylindrical screened inlet 2.13 m dia and 0.61 m wide. A flared bend with a  $\frac{6}{4}$  to 1 contraction ratio then turns the flow through 90 deg into a concentric cylindrical duct with 1.14 m outside diameter and 0.69 m inside diameter which contains the compressor blade rows. Downstream of the compressor there is an annular diffuser, and a cylindrical sliding throttle at the outlet is used to control the throughflow.

The compressor is a single-stage machine with three blade rows: inlet guide vanes (IGV), rotor and stator. There are 38 blades in each of the guide vane rows, and 37 blades in the rotor, giving a space/chord ratio at mid-blade height of 0.99 and 1.02, respectively. The axial row spacings in these tests were 91 mm (1.20 c) IGV-rotor, and 80 mm (1.05 c) rotor-stator. The blades are all 228 mm long, with a constant chord of 76 mm, giving an aspect ratio of 3.0. The blade profile used in the British C4 section (10 percent chord maximum thickness) on a circular arc camber line. The blade sections were designed to give free vortex flow, with 50 percent reaction at mid-blade height at

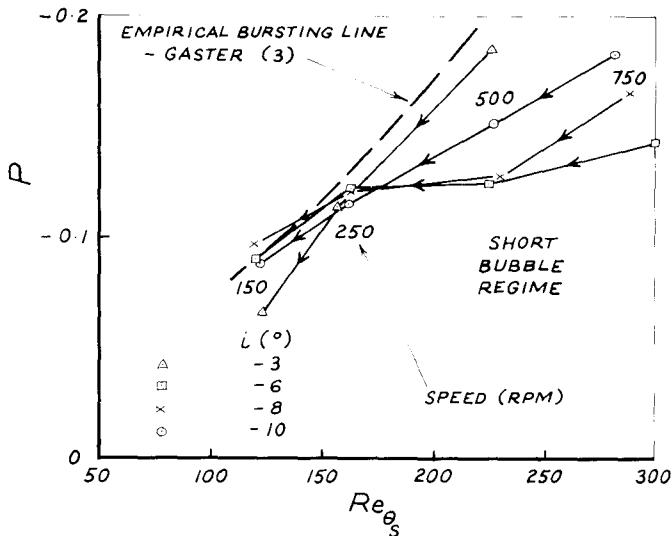


Fig. 7 Trajectories of  $P \sim Re_{\theta_s}$  for laminar separation bubbles on the stator suction surface at negative incidence and comparison with Gaster's bursting criterion

a flow coefficient ( $\nabla_a/U_{mb}$ ) of 0.76. The blade angles at mid-blade height are as follows:

	$\beta_1$ (deg)	$\beta_2$ (deg)
IGV	0.0	27.8
Rotor	45.0	14.0
Stator	45.0	14.0

Instrument slots in the outer shell of the compressor allow for radial and axial traversing of measuring probes at a fixed circumferential position. The IGV and stator rows are each mounted on rotatable supporting rings to permit circumferential traversing of these blades relative to a stationary probe.

#### Laminar Boundary Layer Behavior

Surface Visualisation. Extensive regions of laminar flow were observed on both rotor and stator blades in the compressor despite the high level of free stream disturbance to which blades were subjected. The extent of laminar flow did not differ greatly from that observed on identical blade sections tested in a two-dimensional cascade under low turbulence conditions (6, 7). Laminar flow was observed up to 75 percent of chord on the suction surface of the compressor blades at high negative incidence, and it appeared that the flow could easily have been made entirely laminar by suitable choice of the surface pressure distribution.

Fig. 4 shows a typical result of a china

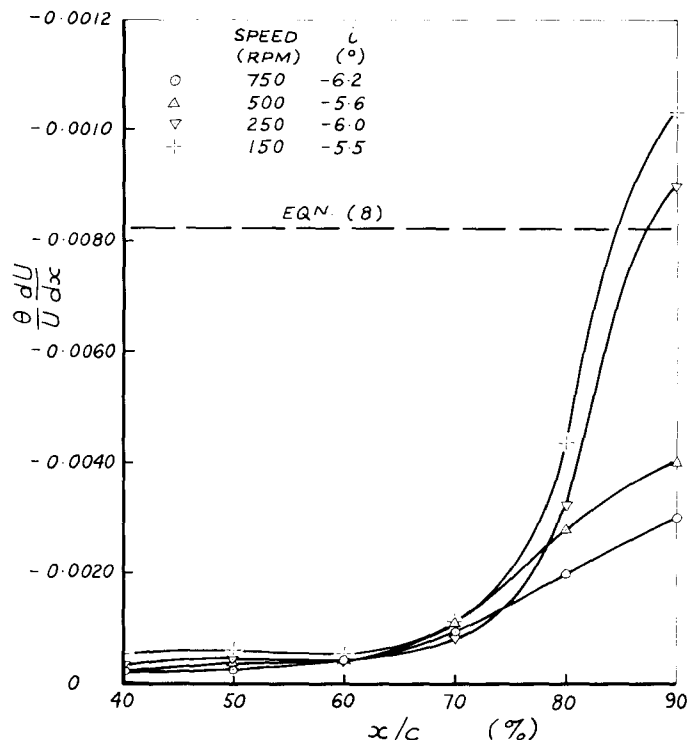


Fig. 8 Variation of pressure gradient parameter  $(\theta/U) (dU/dx)$  on the stator blade suction surface at mid-blade height for  $i \approx -6$  deg (see Table 1) for location of separation, transition and reattachment points)

clay visualization test on the suction surface of a stator blade at moderate negative incidence ( $i = -6.2$  deg at mid-blade). A white drying zone near the leading edge extends to about 30 percent chord; it is followed by a dark region over the central part of the blade where drying is incomplete; finally, there is another more intense drying zone over the rearward part of the blade. This drying pattern indicates the presence, near the leading edge, of a region of accelerating laminar flow with a moderately high wall shear stress; this is followed by a region of decelerating laminar flow, where the wall shear stress is much lower and laminar separation probably occurs; the sudden increase in wall shear stress at the rear of the separation zone is due to the reattachment of a turbulent shear layer, following transition in the separated shear layer.

The line of turbulent reattachment in Fig. 4 is quite sharply defined, and runs almost parallel to the stator trailing edge over most of the blade height, probably because the blade incidence varies little with radial position in this case. Near the stator hub and tip, however,



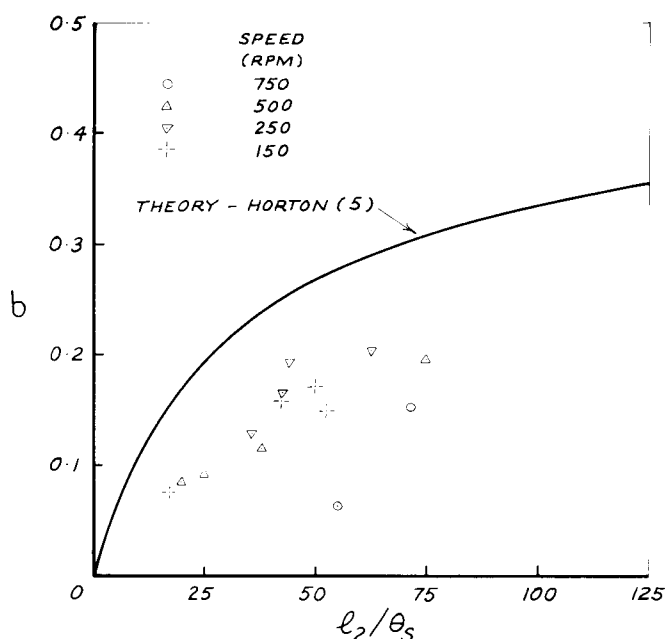


Fig. 9 Variation of pressure recovery parameter with length of turbulent flow in separation bubbles on the stator blade suction surface

the reattachment line curves sharply forward. This effect is most pronounced at the hub, where the secondary flows in the annulus wall boundary layer produce a large streamwise vortex in the corner between the stator suction surface and the hub wall of the compressor. The regions of strong secondary flow on the suction surface occupy 10 to 15 percent of the blade height at the stator hub, and 5 to 10 percent of the blade height at the stator tip; they vary in extent with the blade incidence, being largest near positive stall. There appears to be a rough correlation between the extent of the secondary flow regions and the magnitude of the axial velocity ratios.

Fig. 4 clearly shows a number of white lines of more intense drying, trailing from small isolated roughness elements near the leading edge of the blade. These lines give a rough indication of the direction of the limiting streamlines at the blade surface, and their small radial movement implies that the boundary layer flow near the leading edge is closely two-dimensional over the central 80 percent of the blade height.

Boundary Layer Measurements. The measured values of momentum thickness in laminar boundary layer regions on the stator suction surface were in quite good agreement with the values predicted by Thwaites's method (24) using the measured

surface pressure distributions. The differences between the calculated and measured values of  $\theta$  were about 4 percent, on the average, and seemed to be fairly randomly distributed. Some of these deviations could have arisen from errors in measuring the boundary layer thicknesses and surface velocity distributions; the remainder would have been due to the approximations involved in Thwaites's method, and to departures from the physical model such as three-dimensional and unsteady flow effects. It is interesting to note that the relative differences between the calculated and measured momentum thickness values did not vary significantly with Reynolds number. Values of boundary layer shape factor  $H$  (used to calculate the displacement thickness from  $\delta^* = H\theta$ ) were predicted to about the same accuracy as the momentum thickness. The differences between the measured and predicted values of  $H$  also showed no significant variation with Reynolds number. However, there was a definite tendency for the measured values of  $H$  to fall below the theoretical values immediately upstream of the transition point. This effect, which was particularly notable in the case of a boundary layer measured at  $-3.1$  deg incidence, was probably due to a reduction in displacement thickness generated by the mixing from three-dimensional laminar flow disturbances, or from occasional bursts of turbulence starting to appear in the boundary layer.

An indication of the magnitude of flow convergence effects in these tests was obtained by comparing locally measured momentum thickness values with those obtained by applying the two-dimensional momentum integral equation up to the point in question (using measured values of the appropriate parameters). The departures from the two-dimensional momentum thickness value thus defined, were generally less than 5 percent in regions of attached laminar flow. However, a marked increase in flow convergence effects was noted in separated flow regions.

#### Laminar Separation

The experimental positions of laminar separation on the stator suction surface were taken as the points where the value of boundary layer shape factor,  $H$ , obtained from the hot wire measurements reached 3.70, the critical value adopted by Thwaites (24). These were compared with calculated positions of laminar separation obtained by Thwaites's method, using the measured blade surface velocity distributions,  $U(x)$ . In calculating the separation point, the velocity gradient  $dU/dx$  was obtained by using a

linear fit to the measured values of  $U$  and assuming a discontinuity in  $dU/dx$  to occur at separation.

The hot wire measurements indicated that there was no laminar separation from the stator blade suction surface at small positive incidence (0 to 5 deg), even though the calculated separation point preceded the observed transition point by a few percent of chord. In these cases, separation was apparently suppressed by the mixing from three-dimensional disturbances in the rearward part of the laminar instability region, or from occasional bursts of turbulence which were starting to appear in the boundary layer. Thus, a comparison of the measured and calculated separation points on the stator is only possible for the boundary layers obtained at negative incidence, where the separation regions became fairly well developed.

At the highest Reynolds numbers investigated (corresponding to a compressor speed of 750 rpm), the separation regions on the stator blade were generally less than 10 percent chord in length. The peak values of  $H$  only slightly exceeded the critical value of 3.70, and the measured separation points lay downstream of those calculated from Thwaites's method by 5 to 8 percent of chord. This difference could have been partly due to occasional turbulent mixing delaying separation, and partly due to errors from applying Thwaites's method in a situation where the surface velocity distribution was slightly convex.

At the lower compressor speeds of 500, 250, and 150 rpm, where separation from the stator blade was much more highly developed, the experimental and calculated separation points agreed to within 2 percent of chord in most cases. The good agreement was possibly the fortuitous result of the surface velocity distributions on the stator suction surface at negative incidence being approximately linear in the neighborhood of the separation point. (The approximate functions chosen by Thwaites are a close fit to the exact solutions for a laminar boundary layer in linearly decelerating flow.)

The laminar separation points were also calculated from the modification of Thwaites's method suggested by Curle and Skan (25), and compared with the experimental separation points obtained by using a critical value of  $H = 3.55$ . However, the agreement was significantly poorer, in most cases, than that obtained by using a critical value of  $H = 3.70$ .

China clay tests showed the behavior of separated laminar flow regions on the rotor blade suction surface to be closely similar to

that on the stator over the common incidence range of -11 to 5 deg. At incidences greater than +5 deg (not attainable on the stator), a small well-developed laminar separation bubble was observed to reappear on the rotor suction surface close to the leading edge.

#### Length of Separated Laminar Shear Layer

It is seen from Fig. 1 that the length of separated laminar shear layer in a short laminar separation bubble is approximately equal to the length of the dead air region. Fig. 5 shows the non-dimensional length of the dead air region,  $\ell_1/\theta_S$ , plotted against the boundary layer Reynolds number at separation,  $Re_{\theta_S}$ , for laminar separation bubbles on the suction surfaces of both rotor and stator blades. The experimentally determined separation points defined by  $H = 3.70$  were taken as the upstream limit of the dead air region on the stator blade; for the bubbles on the rotor blade, the separation points calculated from Thwaites's method were used. The point of apparent turbulent flow reattachment obtained from the china clay tests was taken as the downstream limit of the dead air region in all cases.

The china clay drying pattern is related to the evaporation rate of the surface oil-film, which is expected to depend more on the magnitude of the wall shear stress than on its direction. Hence, the vigorous fluctuations in velocity which occur at a mean reattachment point should cause the drying rate there to be quite appreciable, even though the time mean value of the wall shear stress is zero. As there is also likely to be a significant surface drying rate underneath the turbulent flow region in the rear of a separation bubble, the apparent point of reattachment obtained from the china clay tests should indicate the downstream limit of the dead air region under the separated shear layer, rather than the true mean reattachment point. The reattachment point indicated by the china clay tests on the stator blade suction surface generally lay close to the point at which pressure recovery commenced, but well upstream of the reattachment point defined by  $H_R = 3.50$ .

The values of  $\ell_1/\theta_S$ , shown in Fig. 5, do not exhibit any definite variation with  $Re_{\theta_S}$ , and certainly do not follow equation (9), used by Horton (5) to correlate the measurements of Gaster (3) and other workers. Equation (9) can alternatively be written as

$$Re_{\ell_1} = U_S \ell_1 / \nu = 4 \times 10^4 \quad (12)$$

which indicates that the dead air region should occupy an increasingly large proportion of the surface of an aerofoil as the chord Reynolds number,  $Re_c$ , is reduced. In the separation bubbles on the compressor blades, however, the length of the dead air region at a given blade incidence remained essentially constant as the compressor speed was changed by a factor of 5; and whereas equation (12) indicates that the bubbles should have been longer than the blade chord at a compressor speed of 150 rpm, where  $Re_c \approx 3 \times 10^4$ , the measured bubble lengths were only 10 to 30 percent of chord.

Finally, it is interesting to note that, although there is a considerable scatter in the measured values of  $\lambda_1/\theta_s$ , shown in Fig. 5, no major difference between the flow behavior on the rotating and stationary blade surfaces is apparent.

#### Velocity Profiles in Separation Bubbles

The mean velocity profiles measured in separated laminar flow regions on the stator blade suction surface were very similar to the velocity profiles measured by Gaster (3) in separation bubbles generated on a flat plate. No points of zero velocity away from the surface were indicated by the measurements on the stator blade, but this was to be expected because of the probe response to the large velocity fluctuations present in the separation zone. Nevertheless, it was quite common to obtain velocity readings of only 1 to 2 percent of free stream velocity in the area beneath the separated laminar shear layer. It is not possible to deduce from the hot wire readings (obtained with a single wire probe) whether continuous reversed flow was present underneath the separated shear layer in separated flow regions on the compressor blades. But in view of the small mean velocities observed, and the large disturbances associated with the passage of blade wakes, it does seem likely that intermittent forward flow could have existed close to the blade surface in the bubbles obtained at the higher compressor speeds, where laminar separation was not so highly developed.

#### Influence of Separation Bubbles on the Surface Pressure Distribution

The shape of the surface pressure distribution on a body is often used, in the absence of more detailed information, to determine whether regions of flow separation are present on the body surface. Following Fig. 2, it is usually supposed that a separation bubble causes the appearance of a "flat," or region of zero pressure gradient ( $dp/dx = 0$ ). The assumption of zero pressure

gradient over the separated laminar flow region is also an essential part of Horton's model for the short separation bubble, described in a previous section. It is, therefore, of interest to examine the influence of separated laminar flow regions on the compressor blade surface pressure distributions.

Fig. 6 shows the surface velocity distributions  $U(x)$  obtained on the stator suction surface at about -6 deg incidence for the four different compressor speeds investigated; complementary data are given in Table 1. There is a laminar separation bubble starting at about 60 percent chord, which increases in length from 8 to 27 percent of chord, as the compressor speed is decreased from 750 to 150 rpm, giving a corresponding reduction in  $Re_c$  from  $1.72 \times 10^5$  to  $3.24 \times 10^4$ . The resulting perturbations to the surface velocity distribution are confined mainly to the neighborhood of the separation bubble, and there is little change in the shape of the velocity distribution near the leading edge of the blade as the speed is altered.

At  $Re_c = 1.72 \times 10^5$ , there is certainly no flat in the surface velocity distribution in the neighborhood of the separation bubble. Only a slight change in  $dU/dx$  is discernible near the transition point at the downstream end of the bubble, where there is a discontinuity in the rate of growth of the boundary layer displacement thickness. As the blade Reynolds number is reduced, the length of the separation bubble gradually increases, and the separated shear layer is able to move further from the blade surface, as indicated by the higher peak values of  $H = \delta^*/\theta$  obtained from the hot wire measurements. This is accompanied by a gradual flattening of the velocity distribution in the neighborhood of the bubble, but even at the lowest Reynolds number of  $3.24 \times 10^4$  obtained at 150 rpm, a small positive pressure gradient still appears to exist over the separated flow region.

Judging from these measurements, it seems that peak values of  $H = 5$  or  $6$  are required before a true "flat" in the surface pressure distribution will be observed in the neighborhood of a laminar separation bubble. With less well-developed separation, the streamwise pressure gradient over the forward part of a separation bubble should certainly be reduced, but would be unlikely to fall to zero. A separated flow region which is only just commencing to develop (say  $H_{max} = 4$ ) would have such a minor effect on the surface pressure distribution that its presence might not be detected at all if the surface pressure tappings were widely spaced.

- $x_S$  = Laminar separation point from hot wire measurements ( $H = 3.70$ )  
 $x_t$  = Onset of turbulent flow from stethoscope  
 $x_R$  = Turbulent reattachment point from hot wire measurements ( $H = 3.50$ )  
 $x_T^!$  = Point of wholly turbulent flow from stethoscope (\* = indeterminate)

#### Bubble Regime

Taking  $\delta_S^* \approx 4\theta_S$ , it is seen from Fig. 5 that all the separation bubbles on the compressor blades had lengths of  $O[10\delta_S^*]$ . This at first suggests that they fall in the short bubble regime, although it is usually supposed in the literature that short bubbles have lengths of  $O[10^2 \delta_S^*]$ , which is an order of magnitude greater. But whereas short bubbles on isolated aerofoils operating at high Reynolds number usually occupy only 1 percent of chord or so, the separation bubbles on the compressor blade suction surfaces occupy up to 30 percent of chord, which is more typical of the long bubble regime. It is obviously very difficult, if not impossible, to infer the bubble flow regions from the values of such relative length scales.

In an attempt to resolve the question of bubble classification, trajectories of Gaster's parameter,  $P$ , against separation Reynolds number,  $Re_{\theta_S}$ , were plotted for the bubbles formed on the stator suction surface at negative incidence. The results are shown in Fig. 7. Values of  $P$  were calculated using the points of turbulent reattachment defined by Horton's criterion,  $H_R = 3.50$ .

At the highest compressor speed of 750 rpm, all the points in the  $P \sim Re_{\theta_S}$  plane lie in the short bubble regime to the right of Gaster's empirical bursting line. As the compressor speed falls, the bubble trajectories approach the bursting line, and appear to meet it when the speed is a little above 250 rpm; they then turn and follow the bursting line quite closely as the speed drops from 250 to 150 rpm. This behavior is very similar to that observed by Gaster (3) in his Series II tests, and suggests that the bubbles occurring at 750 and 500 rpm are "short" bubbles, while those at 250 and 150 rpm should be classified as "long" bubbles.

It is seen from Table 1 that turbulent reattachment occurs within 2 percent of chord from the transition point in the short bubbles obtained at 750 and 500 rpm. With a fall in compressor speed to 250 rpm, the distance from transition to reattachment suddenly increases by about 10 percent of chord, but there is little further change in this distance as the speed is reduced to 150 rpm. The sudden change in reattachment

behavior between 500 and 250 rpm seems to confirm that bubble bursting occurs somewhere within this speed range.

Table 1 also shows that the transition point in the separated shear layer remains almost stationary as bursting of the separation bubble occurs. This is in agreement with the observation of Woodward (22), and reinforces the view that bubble bursting is related to the turbulent reattachment process, rather than to the stability of the laminar shear layer.

Accepting that the bubbles formed at 250 and 150 rpm are, in fact, long bubbles, it is noteworthy that their non-dimensional lengths,  $\lambda/\delta_S^*$ , are two or three orders of magnitude smaller than the values suggested by Owen and Klanfer (18). Another interesting feature is that the appearance of a long bubble on the rearward part of the stator suction surface does not cause the marked collapse in the suction peak which is commonly observed when a long bubble is formed close to the leading edge of an isolated aerofoil (see Fig. 2). Although the non-dimensional velocity distributions, shown in Fig. 6, differ significantly over the forward 60 percent of the stator suction surface, these variations are very largely explained by small changes in the axial velocity and blade incidence. The velocities in Fig. 6 are made non-dimensional with respect to the mid-blade rotor velocity,  $U_{mb}$ , and the flow coefficient,  $\bar{V}_a/U_{mb}$ , changes slowly with compressor speed. Thus, in this particular case, the perturbation of the surface pressure distribution caused by the long bubble formation, is mostly a displacement effect which is confined to the neighborhood of the bubble.

The formation of a long bubble on the rearward part of an aerofoil must, of course, affect the pressure distribution near the leading edge to some extent, as the change in boundary layer thickness accompanying its appearance will shift the trailing edge separation point, and so alter the circulation around the aerofoil. However, it appears that such circulation changes need not be very large, unless the location of the bubble does not permit the full pressure rise during reattachment to be achieved before the trailing edge is reached.

#### Turbulent Shear Layer Behavior

At a compressor speed of 750 rpm, where the laminar separation bubbles on the stator suction surface at negative incidence were not very well developed, the point of wholly turbulent flow,  $x_T^!$ , occurred well downstream of the separated flow region; in this case, the separated

shear layer was able to reattach while only intermittently turbulent. As the compressor speed was reduced, the value of  $H$  at the point of wholly turbulent flow gradually increased until it eventually exceeded 3.50, indicating that transition had been completed before reattachment occurred. At a speed of 250 rpm, transition occurred entirely within the separated shear layer in at least two cases ( $i = 8.0$  deg and  $-10.1$  deg); here it seemed that continuous turbulent mixing was required to enable the separated shear layer to reattach.

The behavior of the turbulent shear layer in separation bubbles observed on the stator suction surface at  $i \approx -6$  deg has been indicated in Table 1. A very similar behavior was observed by Gaster (3), who noted that the turbulent mixing region occupied an increasingly large proportion of a laminar separation bubble on a flat plate as the tunnel speed was reduced.

To examine the validity of Horton's turbulent reattachment criterion,  $[(\theta/U) (dU/dx)]_B = -0.0082$ , the measured variation of  $(\theta/U) (dU/dx)$  on the stator suction surface at about  $-6$  deg incidence has been presented in Fig. 8. Curves have been plotted for each of the four different compressor speeds investigated. At the point of reattachment behind the short bubbles obtained at speeds of 750 and 500 rpm,  $(\theta/U) (dU/dx)$  attains values of only  $-0.001$  to  $-0.002$ , which are significantly smaller than the values suggested by Horton. The values observed on the compressor blades are not necessarily inconsistent with Horton's model, however, as the reattaching shear layer is only intermittently turbulent in these particular cases, and would, therefore, be expected to have a lower time mean value of the dissipation coefficient than a fully turbulent layer. According to Horton's theory, equation (4), this should lead in turn to a smaller value of  $(\theta/U) (dU/dx)$  at the reattachment point.

In the long separation bubbles obtained at 250 and 150 rpm, the flow is essentially fully turbulent at the point of reattachment for  $i = -6$  deg. Here,  $(\theta/U) (dU/dx)$  takes values in the range  $-0.009$  to  $-0.010$  which agrees reasonably well with the value of  $-0.0082$  suggested by Horton. Very similar values of  $(\theta/U) (dU/dx)$  were obtained behind long bubbles on the stator suction surface at other negative values of blade incidence. The agreement with Horton's model is within the range of experimental error, considering that  $dU/dx$ , which varies rapidly with  $x$  near reattachment, was determined from values of  $U$  measured at 10 percent intervals of chord. However, it is noteworthy that the values of  $(\theta/U) (dU/dx) \approx -0.0010$  obtained behind long bubbles on the compressor

blades are in general agreement with the long bubble data analysed by Horton.

#### Pressure Rise During Turbulent Reattachment

Provided that the shear layer is fully turbulent over the length,  $l_2$ , of the pressure recovery region at the rear of a separation bubble, the assumption of a linear surface velocity distribution during reattachment (Fig. 3), together with a value of  $(\theta/U) (dU/dx) = -0.0082$  at the reattachment point, leads to a unique relationship between the non-dimensional pressure rise over the bubble,  $\sigma$ , and the non-dimensional length,  $l_2/\theta_S$ . This relation, which forms the basis of Horton's bubble bursting theory, is reproduced in Fig. 9, together with the measured values of pressure rise in separation bubbles on the stator blade suction surface. In calculating values of  $l_2$  for the bubbles on the compressor blade, the pressure recovery was assumed to commence at the point of apparent turbulent reattachment obtained from the china clay tests, as this approximates the downstream limit of the dead air region in which the surface pressure remains nearly constant. (Inspection of the blade surface velocity distributions showed that at negative incidence there was usually a sudden increase in pressure gradient within 3 or 4 percent chord downstream of the china clay reattachment point.) The downstream end of the pressure recovery region was defined as the point where the measured value of  $H$  fell to 3.50.

It is seen from Fig. 9 that, although the measurements show a similar trend to the theory, the streamwise distance required to achieve a given pressure rise on the compressor blade is at least double that predicted by Horton. This difference is considered significant in spite of the possible errors of at least 50 percent in determining  $l_2$ . The present observations do not completely invalidate Horton's theory, however, as the reattaching shear layers on the compressor blade are only intermittently turbulent, while the theoretical model assumes the flow to be fully turbulent. A reduction in the mean rate of entrainment by the shear layer would be expected to increase the distance to reattachment, and there is, in fact, a notable tendency for the values of  $l_2/\theta_S$  to be greater at the higher compressor speeds, where the intermittency of turbulence and the magnitude of  $(\theta/U) (dU/dx)$  at reattachment are both much lower.

It is interesting to note that in the short separation bubbles obtained on the stator suction surface at compressor speeds of 750 and 500 rpm, the point of reattachment indicated by the china clay tests was, on average, almost identical with the point at which turbulent flow was

first observed with the stethoscope. This agrees fairly well with Horton's model of the flow in a short separation bubble (Fig. 3), which assumes that the length of the constant pressure region is approximately equal to the length of the separated laminar shear layer, and that pressure recovery commences at the transition point. In the long bubbles obtained at 250 and 150 rpm, however, the transition point was consistently 4 to 5 percent of chord upstream of the china clay reattachment point, and the length of the (approximately) constant pressure region was at least 50 percent greater than the length of the separated laminar shear layer. The assumption that pressure recovery commences at the transition point in a long bubble would, therefore, lead to a serious underestimation of the total bubble length.

#### MODIFICATIONS TO HORTON'S MODEL

##### Introduction

The foregoing discussion has indicated that some of the empirical correlations used by Horton (5) are not sufficiently general to give an accurate description of the separation bubble behavior on the compressor blades. In particular, equation (9) overestimates the length of the constant pressure region at low Reynolds numbers, and equation (8) underestimates the length of the pressure recovery region when the reattaching shear layer is not fully turbulent. The assumption of constant pressure over the separated laminar flow region is also open to question.

Some modifications to these correlations will now be proposed in order to improve the predictions of bubble length given by Horton's model. The problem of allowing for a variation in pressure over the separated laminar flow region will not be discussed, as this would involve a detailed consideration of external flow interactions which would mean abandoning Horton's simple type of model entirely.

##### Length of the Constant Pressure Region

The length,  $l_1$ , of the constant pressure region in a laminar separation bubble is basically dependent on the location of the transition point in the separated laminar shear layer. The transition point, in turn, is determined by the amplification of disturbances in both the attached laminar boundary layer and the separated shear layer. If the surface pressure distribution upstream of the laminar separation point is arbitrary, the length of the constant pressure region cannot, in general, depend entirely on the local conditions at sepa-

ration, as implied by equation (9). The only physically realistic method of predicting the length of separated laminar flow in a bubble is, therefore, to employ a correlation giving the entire length of unstable laminar flow (i.e., the distance,  $l_1$ , from the point of neutral stability,  $x_i$ , in the attached boundary layer to the transition point  $x_t$  where turbulence first appears in the separated shear layer).

The writer (26) has found the correlation

$$(Re_{\theta_t} - Re_{\theta_i})/Re_{\theta_m} = 1.70 - 0.32 H_m \quad (13)$$

to describe the transition behavior on several different aerofoil sections under a wide range of conditions. An alternative form of this correlation is

$$(l_1/\theta_m)/Re_{\theta_m} = (0.606 H_m - 0.414)/(H_m - 2.29) \quad (14)$$

where the subscript, m, denotes a mean value over the region of unstable laminar flow. Equation (14) successfully describes the transition behavior in flows with both short and long separation bubbles on the compressor blades, and is also a reasonable fit to the data from Gaster's Series II measurements of separation bubbles generated on a flat plate (3). The values of instability length show an average deviation of some 10 percent from the mean curve given by equation (14). This correlation should at least give a good qualitative description of the laminar separation bubble behavior, and it should be more generally applicable than equation (9) which it replaces.

Woodward (4) has also noted the failure of correlations, such as equation (9), to give a generally accurate description of the length of laminar flow in a separation bubble. Woodward's work indicated that the length of the laminar shear layer could be represented in a number of cases by the relation

$$l_1/\theta_S = A Re_{\theta_S} + B/Re_{\theta_S} \quad (15)$$

where A and B are both functions of the imposed pressure distribution. It is noted that the  $A Re_{\theta_S}$  term in equation (15) is qualitatively consistent with the transition correlation given by equation (14).

No allowance for the effects of free stream turbulence or unsteadiness has been suggested in the foregoing transition correlations. The influence of free stream disturbances on transi-

tion, where significant, depends on so many factors that no generally valid correlation of their effect is likely to be obtained. Equations (13) and (14) correlate data from tests with turbulence levels ranging from near zero to over 6 percent, and this indicates that free stream disturbances have only a minor direct influence on the transition process on an aerofoil in a great many cases. There will, of course, be some situations where free stream disturbances have a marked influence on transition, notably where the suction peak location on a body is very sensitive to incidence change. The use of equations (13) and (14) will then significantly overestimate the length of unstable laminar flow. A fuller discussion of the effects of free stream disturbances on transition can be found in References (27) and (28).

#### Length of the Pressure Recovery Region

It appears that Horton's model of the reattachment process should provide an adequate estimate of the distance between the end of the constant pressure region, and the reattachment point when the separation bubble is sufficiently well-developed for the shear layer to be fully turbulent over most of the pressure recovery region. If the shear layer is only intermittently turbulent at the reattachment point, however, the distance to reattachment will be seriously underestimated. In the latter case, some modification of Horton's method is required to take into account the lower dissipation coefficient of the partly turbulent flow, which leads to a smaller value of  $(\theta/U)(dU/dx)$  at reattachment. It is suggested that even a crude model, such as the assumption of a linear variation of eddy viscosity over the length of the transition region, would lead to greatly improved agreement with experiment.

The inadequacy of Horton's point transition model in the case of separation bubbles on the compressor blades is readily apparent from the data in Table 1. This shows that the length of intermittently turbulent flow on the compressor blade was typically about 15 percent of chord. The large extent of the transition region is thought to have been caused by free stream unsteadiness associated with the passage of blade wakes, as discussed in Reference (27).

#### CORRELATIONS FOR THE CRITICAL REYNOLDS NUMBER OF AN AXIAL COMPRESSOR CASCADE

The sudden increase in losses of an axial compressor cascade, which occurs as the Reynolds number is reduced below a certain critical value, is associated with the bursting of laminar separa-

tion bubbles on the blade surfaces. Roberts (13) has proposed an empirical correlation of the bursting Reynolds number,  $Re_b$ , in terms of the overall diffusion factor,  $D$ , by means of the relation

$$Re_b = (1.83D + 0.8) \times 10^5 \quad (16)$$

which was obtained from tests on cascades of NACA 65-series blades with an inlet turbulence level of about 0.5 percent. Equation (16) which is broadly analogous to Gaster's bursting criterion based on local flow parameters, indicates that  $Re_b$  should increase as the diffusion factor (and, hence, lift coefficient) is increased.

Correlations such as equation (16), however, can only be expected to be valid for a limited class of surface pressure distributions. It is the relative variation of  $\theta$  and  $dU/dx$  for the reattaching turbulent shear layer which determines the behavior of  $Re_b$ , and this, in turn, depends on the nature of the surface pressure distribution. The work of Howard et al. (6-8) on blading with different forms of surface pressure distribution showed that a wide range of  $Re_b$  values could be obtained with the same values of  $D$  and inlet turbulence;  $Re_b$  was generally increased by moving the suction peak rearwards. These results are clearly in conflict with the predictions of equation (16). Another series of tests by Rhoden (9) on British C4 circular arc cambered blades showed a considerable operating range over which  $Re_b$  fell with increase in  $D$ ; this trend is the reverse of that indicated by equation (16).

Woodward (4) has made similar comments about the general validity of Gaster's bursting criterion. He noted that the bursting boundary indicated by tests on NACA 66<sub>3</sub>-018 and 0010 aerofoil sections appeared to differ significantly from that proposed by Gaster.

As regards the influence of free stream disturbances on the critical Reynolds number for a cascade, the experimental evidence indicates that an increase in turbulence level will generally cause a fall in  $Re_b$  through promoting earlier transition in the separated shear layer. It should be noted, however, that only small movements of the transition point are usually required to produce these performance changes. The influence of free stream disturbances on transition is very complex, and depends on a number of factors including the surface pressure distribution. With many types of surface pressure distribution, the influence of turbulence on transition may be quite small; with others it can be quite large

[see Reference (28) for a fuller discussion]. Correlations of bursting behavior in terms of the free stream turbulence properties alone are, therefore, unlikely to be generally valid. Robert's (13) tentative correlation for the influence of turbulence on the bursting Reynolds number of an axial compressor cascade certainly does not describe the whole range of behavior observed in the tests of References (6-15).

#### SUMMARY

Previous work on the growth and bursting of laminar separation bubbles has been reviewed. Some detailed observations of laminar separation bubble behavior on the blading of an axial compressor have been presented. On the basis of these measurements, some modifications to Horton's semi-empirical theory for the growth and bursting of laminar separation bubbles have been suggested. Finally, it has been stressed that correlations of the critical Reynolds number for axial compressor cascades should be applied with extreme caution, since they are only likely to be valid for a narrow range of conditions.

#### ACKNOWLEDGMENTS

This work was supported by grants from the Australian Department of Supply, whose assistance is gratefully acknowledged.

#### REFERENCES

- 1 Tani, I., "Low Speed Flows Involving Bubble Separations," *Progress in Aeronautical Science*, Vol. 5, Pergamon, 1964.
- 2 Young, A. D., and Horton, H. P., "Some Results of Investigations of Separation Bubbles," *North Atlantic Treaty Organisation, AGARD C.P. No. 4*, 1966, pp. 779-811.
- 3 Gaster, M., "The Structure and Behavior of Laminar Separation Bubbles," *United Kingdom, National Physical Laboratory, Aero. Report No. 1181 (Revised)*, March 1967.
- 4 Woodward, D. S., "An Investigation of the Parameters Controlling the Behaviour of Laminar Separation Bubbles," *United Kingdom, Royal Aircraft Establishment, Tech. Memo, Aero. 1003*, Aug. 1967.
- 5 Horton, H. P., "A Semi-Empirical Theory for the Growth and Bursting of Laminar Separation Bubbles," *United Kingdom, Aeronautical Research Council, Current Paper No. 1073*, 1969.
- 6 Blight, F. G., and Howard, W., "Tests on Four Aerofoil Cascades. Part 1: Deflection,

Drag and Velocity Distribution," *Australian Department of Supply, Aeronautical Research Laboratories, Report E74*, July 1952.

- 7 Blight, F. G., and Howard, W., "Tests on Four Aerofoil Cascades. Part 11: Boundary Layer Characteristics," *Australian Department of Supply, Aeronautical Research Laboratories, Report E75*, July 1952.

- 8 Crooks, P. V., and Howard, W., "Low Speed Tests on Three Aerofoil Cascades Designed for Prescribed Surface Velocity Distributions," *Australian Department of Supply, Aeronautical Research Laboratories, Report ME 76*, June 1954.

- 9 Rhoden, H. G., "Effects of Reynolds Number on the Flow of Air through a Cascade of Compressor Blades," *United Kingdom, Aeronautical Research Council, Reports and Memoranda No. 2919*, June 1952.

- 10 Stuart, D. J. K., "Analysis of Reynolds Number Effects in Fluid Flow through Two-Dimensional Cascades," *United Kingdom, Aeronautical Research Council, Reports and Memoranda No. 2920*, July 1952.

- 11 Citavy, J., and Norbury, J. F., "The Effect of Reynolds Number and Turbulence Intensity on the Performance of a Compressor Cascade with Prescribed Velocity Distribution," *University of Liverpool, Department of Mechanical Engineering Report*, Oct. 1973.

- 12 Schlichting, H., "Recent Progress in Boundary Layer Research," *American Institute of Aeronautics and Astronautics Journal*, Vol. 12, No. 4, Apr. 1974, pp. 427-440.

- 13 Roberts, W. B., "The Effect of Reynolds Number and Laminar Separation on Axial Cascade Performance," *American Society of Mechanical Engineers, Paper No. 74-GT-68*, 1974.

- 14 Shaw, R., "The Effects of Reynolds Number, Turbulence Intensity and Axial Velocity Ratio on Compressor Blade Performance," *Proceedings of Institution of Mechanical Engineers*, Vol. 184, part 3G (11), 1969-1970, pp. 93-100.

- 15 Walker, G. J., "An Investigation of the Boundary Layer Behavior on the Blading of a Single-Stage Axial-Flow Compressor," *Ph.D. Thesis, University of Tasmania*, Nov. 1971.

- 16 Walker, G. J., "The Prediction of Boundary Layer Development on Axial Flow Turbomachine Blades," *Proceedings of Third Australasian Conference on Hydraulics and Fluid Mechanics*, Sydney, Nov. 1968, pp. 97-104.

- 17 Evans, B. J., "Effects of Free-Stream Turbulence on Blade Performance in a Compressor Cascade," *Cambridge University Engineering Department /A, Report Turbo./TR. 26*, 1971.

- 18 Owen, P. R., and Klanfer, L., "On the



Laminar Boundary Layer Separation from the Leading Edge of a Thin Aerofoil," United Kingdom, Aeronautical Research Council, Current Paper No. 220, 1955.

19 Crabtree, L. F., "The Formation of Regions of Separated Flow on Wing Surfaces," United Kingdom, Aeronautical Research Council, Reports and Memoranda No. 3122, 1959.

20 McGregor, I., "Regions of Localised Boundary Layer Separation and Their Role in the Nose-Stalling of Aerofoils," Ph.D. Thesis, Queen Mary College, University of London, 1954.

21 Wallis, R. A., "The Turbulent Boundary Layer on the Articulated Nose of a Thin Wing Provided with Air Jets," Australian Department of Supply, Aeronautical Research Laboratories, Note A141, 1954.

22 Woodward, D. S., Unpublished Note, Queen Mary College, University of London.

23 Oliver, A. R., "Comparison Between Sand Cast and Machined Blades in the Vortex Wind Tunnel," Australian Department of Supply, Aero-

nautical Research Laboratories, Report ME 103, Sept. 1961.

24 Thwaites, B., "Approximate Calculation of the Laminar Boundary Layer," Aeronautical Quarterly, Vol. 1, 1949, pp. 245-280.

25 Curle, N., and Skan, S. W., "Approximate Methods for Predicting Separation Properties of Laminar Boundary Layers," Aeronautical Quarterly, Vol. 8, 1957, pp. 257-268.

26 Walker, G. J., "An Investigation of Boundary Layer Transition on an Axial-Flow Compressor Blade," Australian Department of Supply, Aeronautical Research Laboratories, Report ME 122, July 1968.

27 Walker, G. J., "The Unsteady Nature of Transition on an Axial-Flow Compressor Blade," American Society of Mechanical Engineers, Paper No. 74-GT-135, 1974.

28 Walker, G. J., "A Family of Surface Velocity Distributions for Axial Compressor Blading and their Theoretical Performance," Paper submitted for American Society of Mechanical Engineers 1975 International Gas Turbine Conference.